JOURNAL OF OPTOELECTRONICS AND AVANCED MATERIALS Vol. 8, No. 6, December 2006, p. 2058 - 2065

Giant photo-expansion in chalcogenide glass

K. TANAKA*, A. SAITOH, N. TERAKADO
Department of Applied Physics, Graduate School of Engineering, Hokkaido University, Sapporo 060-8628, Japan

Glass exhibits many kinds of photoinduced phenomena, among which the giant photo-expansion appearing in chalcogenide glasses such as As_2S_3 may be the most dramatic and promising. Its feature, mechanism, and application including micro-lenses are described.

(Received October 11, 2006; accepted November 2, 2006)

Keywords: Chalcogenide glass, Photoinduced phenomena, Photo-expansion, Micro-lens

1. Introduction

The glass is known to exhibit a variety of radiation effects. The most famous may be the defect formation and radiation compaction (Table 1) in silica glass [1], which is now commercially utilized for producing Bragg-grating fibers [2]. However, since the oxide glass has a wide bandgap of 4-9 eV and the structure is comparatively rigid, intense pulsed lasers or ultra-violet sources are needed for inducing these phenomena. On the other hand, the chalcogenide glass has a bandgap of 1-3 eV and flexible structures [3,4], and accordingly, it exhibits many kinds of prominent photoinduced phenomena, for which extensive studies have been performed since ~1970 [5,6].

We here focus upon photoinduced volume changes in chalcogenide glasses. It is known that As_2S_3 films, which are prepared through vacuum evaporation, exhibit irreversible volume *contraction* (densification) of ~1% when illuminated with bandgap illumination of $\hbar\omega \geq 2.4$ eV ($= E_g$) (see, Table 1) [7]. This densification is ascribed to relaxational photo-polymerization [8], and accordingly, it cannot be reversed by any means. On the other hand, Hamanaka et al. have discovered that bandgap illumination upon annealed As_2S_3 films and bulk samples produces photoinduced volume *expansion* of ~0.4% [9], which can be recovered with annealing at the glass-transition temperature of ~ 200 °C. This expansion occurs with photodarkening, a parallel red-shift of optical absorption edge, of ~ 30 meV [10] and with refractive-index *increase* of ~ 0.03 [11]. However, more recently, Hisakuni and Tanaka have demonstrated for annealed As_2S_3 films and bulk samples that 2.0 eV sub-gap photons can induce greater volume expansions of ~5%, which can be referred to as *giant* due to its prominence [12].

Table 1. Typical photoinduced changes in volume ΔV and Δn in bulk SiO_2 glass, as-evaporated As_2S_3 film, and bulk As_2S_3 glass. The changes in bulk glasses can be recovered with annealing.

	$\Delta V/V$ (%)	$\Delta n/n$ (%)	Δn	n
SiO_2 (bulk)	-0.001	$+10^{-3}$	$+10^{-5}$	1.5
As_2S_3 (as-evaporated)	-1	+4	+0.1	2.6
As_2S_3 (bulk)	+0.4	+1	+0.02	2.6

The giant photo-expansion has evoked vivid interest in the mechanism and application. Why can only the photon produce such a drastic volume expansion? Why can less-energetic photons by 0.4 eV than the optical gap of 2.4 eV produce greater changes by ten times than that by bandgap illumination? On the other hand, this phenomenon appears to be readily applicable to producing optical devices as micro-lenses. What are practically promising?

In the present work, we will review the giant photo-expansion from fundamental and applied viewpoints. Note that anisotropic deformations [13-15] produced by polarized light are not dealt here. Photoinduced volume expansions and surface-shape modifications in Ag-chalcogenide glasses such as Ag-As-S [16] is neither included, because the phenomenon seems to be caused by a different mechanism of photoinduced Ag^+ ion migration [14].

2. Giant photo-expansion

When a covalent chalcogenide glass is illuminated with focused relatively-intense un-polarized sub-gap light with photon energy of $\hbar\omega \simeq 0.8E_g$, the glass undergoes a prominent volume expansion [12]. For instance, as shown

in Fig. 1, an As_2S_3 glass (E_g = 2.4 eV) flake with a thickness of 50 μm illuminated for 10^3 s by focused 2.0 eV light with intensity of 10^3 W/cm^2, which is obtained from conventional He-Ne lasers, exhibits a volume expansion ΔV with a height ΔL of ~2 μm. This magnitude corresponds to a fractional change of ~5% if normalized by the sample thickness, which is about ten times as great as that (~0.4%) induced by bandgap illumination [9,10]. Three characteristics, obtained for As_2S_3, are worth to be mentioned.

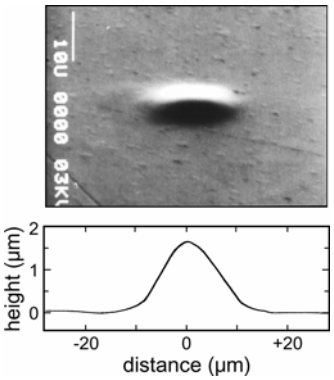

Fig. 1. A photo-expanded As_2S_3 flake, the photograph being taken by a scanning electron microscope (upper), and its surface profile (lower). In this example (when the sample is thinner than ~100 μm), a smaller expansion appears also on the rear surface.

First, the photon energy and the intensity of light are important. As shown by solid circles (intense light) in Fig. 2, the photon energy must lie in the exponential Urbach-edge region of 1.9 - 2.3 eV [17,18], which exists below the Tauc gap of 2.4 eV [3,4]. In addition, as shown in Figs. 2 and 3, the light intensity should be around 10^3-10^4 W/cm^2 [17]. Weaker Urbach-edge light than 10^2 W/cm^2 can induce only optical changes as the photodarkening and related refractive-index increase [17]. On the other hand, more intense light than 10^6 W/cm^2 causes thermal effects such as thermal runaway, melting, and ablation [20,21]. Otherwise, we can employ pulsed light for experiments (Fig. 2) [18,22]. As for the spectral dependence, photons with smaller energies than ~1.5 eV cannot produce appreciable changes under limited light intensities (if nonlinear excitation is neglected [19]). On the other hand, weak bandgap illumination of ~2.4 eV (≲0. 1 W/cm^2) induces the conventional volume expansion of ~0.4% [9,10]. In Fig. 2, the expansion reductions at $\hbar\omega > E_g$ are due to light-penetration effects. It is surprising that *moderate-intensity Urbach-edge light can provide more prominent volume expansions* than that induced by bandgap illumination.

Second, as shown in Fig. 4, the expansion occurs with a photodarkening, but with different time scales [23]. The photodarkening accompanies an *increase* in the refractive index, as is expected from the Kramers-Krőnig relation. Note that the volume expansion accompanying the refractive-index increase is not inconsistent with the Lorentz-Lorenz relation, because the photodarkening suggests a polarisability increase. These volume and optical changes can be erased with annealing at the glass-transition temperature (~200ºC in As_2S_3) [16,23].

Third, as shown in Fig. 5, the glass yields greater expansions upon illumination at lower temperatures [24,25]. An As_2S_3 sample illuminated at 10 K has expanded by ~20 μm [24], which can actually be seen by naked eyes. Note that several observations such as this temperature dependence strongly suggest that the expansion occurs through athermal processes, which is reasonable due to small, but finite, absorptions at Urbach-edge regions, e.g. $\alpha \approx 1$ cm^{-1} at $\hbar\omega$ = 2.0 eV [3,4].

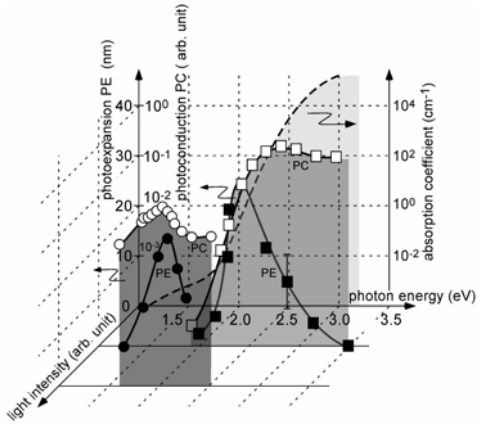

Fig. 2. Spectral dependences of absorption coefficient (dashed line), photoinduced expansions PE (solid symbols), and photocurrents PC (open symbols) in As_2S_3. The expansion and current spectra are measured under 10 mW/cm^2 cw light (squares) and pulsed 10^8 W/cm^2 light (circles) [18].

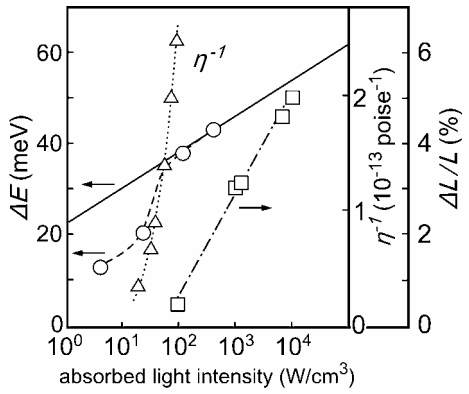

Fig. 3. Light-intensity dependences of some photoinduced changes in As_2S_3 [17,26]. The absorbed light intensity on the horizontal axis is estimated as the product of absorption coefficients and incident cw light intensities. The solid and dashed (with circles) lines show the photodarkening ΔE induced, respectively, by bandgap (2.4 eV) and sub-gap illumination (2.0 eV). Triangles and squares are the changes produced by 2.0 eV light in the fluidity η^{-1} under illumination and in the fractional expansion $\Delta L/L$ after prolonged illumination.

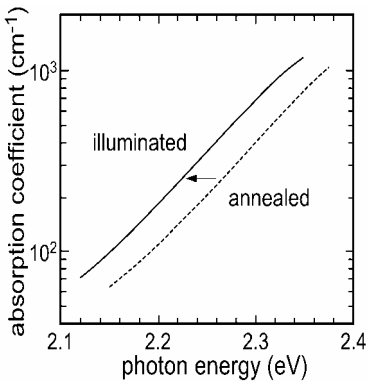

Fig. 4. Photodarkening in an As_2S_3 flake (50 μm thick) induced by an exposure of focused He-Ne laser light (100 W/cm^2) for 1 h. Dependence of the photodarkening on light intensity is shown in Fig. 3.

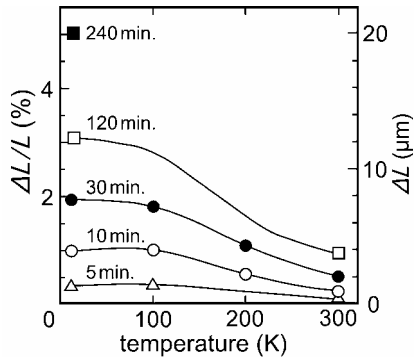

Fig. 5. Temperature dependence of the expansion in an As_2S_3 flake (~400 μm thick) as a function of exposure times indicated [24]. The horizontal axis shows the temperature at which the sample is illuminated. The expansion height ΔL (vertical axes) is measured at room temperature. The exposure is provided from a He-Ne laser of 20 mW, which is focused onto a spot with a diameter of ~50 μm.

Material dependence is also interesting. Volume expansions of a few percent appear in other chalcogenide glasses as As_2Se_3 (E_g ≈1.8 eV), $GeSe_2$ (E_g ≈2.2 eV), and GeS_2 (E_g ≈3.2 eV) when exposed at room temperature to Urbach-edge light of, respectively, $\hbar\omega$ = 1.6, 2.0, and 2.7 eV with moderate intensities [23]. This result is consistent with the known effects induced by bandgap illumination [10]. Accordingly, the photo-expansion seems to be inherent to covalent chalcogenide glasses. Note that, among these glasses, electrons are more mobile only in $GeSe_2$, which means that the expansion is irrespective of the electrical conduction type.

In other materials, studies remain or no clear expansions occur. In pure amorphous Se, if the expansion occurs has not been known due to its low glass-transition temperature of ~30ºC [3,4]. Behaviors in telluride glasses remain to be investigated, and those in Na-Ge-S glasses are unclear [27]. In contrast, in the corresponding crystals of As_2S_3 (orpiment) and GeS_2 (layer-type), no photoinduced changes have been detected. GeO_2 shows photoinduced volume expansion [28], while no giant expansion has been detected upon sub-gap illumination. It is also mentioned that Sramek et al. recently report that some halide glasses containing ZrF_4 exhibit photoinduced volume expansions [29], for which further studies will be interesting. These observations suggest, at the present stage, that the giant photo-expansion appears to be inherent only to the glassy state of covalent chalcogenides. However, quantitative comparisons of the expansion in different glasses under normalized illumination conditions remain to be studied [23].

3. Phenomenological model

A quantitative evaluation of the giant photo-expansion has suggested that this phenomenon appears through two processes, volume expansion and fluidity [12]. That is, as illustrated in Fig. 6, the giant photo-expansion occurs if the intrinsic volume expansion of a_0 (≈ 0.5% [9]), which is isotropic, can be transferred through the photoinduced fluidity [26,30,31] to an expansion at free surfaces. This idea predicts that the expansion with a height ΔL is given as $\Delta L/L = a_0 (1 + L/r)$, where L is sample thickness (when it is smaller than α^{-1}) or effective penetration depth α^{-1} of sub-gap light and r is the light-spot radius. In other words, the giant photo-expansion occurs because the intrinsic volume expansion of a_0 is seemingly amplified by a geometrical factor L/r, which can become greater than unity for focused Urbach-edge light due to the long penetration depth α^{-1} up to ~1 cm [3,4]. In contrast, bandgap light has smaller penetration depths of $\alpha^{-1} \leq 10$ μm [3,4], and accordingly, the photo-expansion is governed by the intrinsic value of a_0 [9,10].

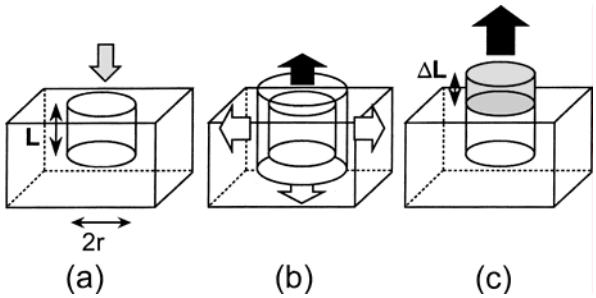

Fig. 6. Schematic illustrations of the giant photo-expansion. (a) Illumination of light with a spot diameter 2r and a penetration length L is initiated. (b) The illuminated volume tends to expand with some mechanism, in which only the expansion toward the free surface (black arrow) may appear. (c) However, if the stress toward unilluminated regions can be relaxed with the photoinduced fluidity, a giant photo-expansion ΔL appears on the surface. If a sample is thinner than L, an expansion also appears on a rear surface.

Therefore, to understand more deeply the giant photo-expansion, we should reveal microscopic mechanisms of the photoinduced volume expansion and the fluidity. Since the latter phenomenon has been reviewed recently [26,31], we will focus upon the expansion.

4. Microscopic mechanism

In general, a photoinduced phenomenon occurs through a series of photo-electro-structural processes [1]. In conventional crystalline semiconductors, bandgap photons excite electron-hole pairs, while the pairs are liable to spatially extend. Then, through electron-phonon coupling the electronic energy may be transferred to lattice vibrations, giving rise to only the temperature rise. The energy flow in this case can schematically be expressed as;

photon → electron-hole → lattice vibration → temperature rise.

On the other hand, in disordered materials and molecular systems, the electronic excitation can be localized, which may be efficiently transferred to atomic structural changes through strong electron-lattice (polaronic) coupling. After the structural change, the electron-hole will recombine. In this case, the light energy can flow as;

photon → electron-hole → atomic change (defect → volume change) and frozen-in.

Therefore, the photo-structural change can be divided into the two processes, which are photo-electronic (4.1.) and electro-structural (4.2.).

4.1 Photo-electronic excitation

For the photo-electronic process, the most puzzling problem in the giant photo-expansion is why the low-energy photon can excite electrons (or holes). In the above, we have seen that the long penetration depth of Urbach-edge light is a prerequisite for bulky excitation. However, why can such less energetic light of $\hbar\omega$ = 2.0 eV than the Tauc gap of 2.4 eV induce photo-electronic excitation? The energy deficiency of ~0.4 eV is substantially greater than the thermal energy of ~25 meV at room temperature. For instance, we note that $\exp(-0.4/0.025) = 10^{-7}$. Moreover, the expansion increases at low temperatures (Fig. 5), where the thermal energy can be practically neglected.

At least, two possibilities can be speculated. One is the two-photon absorption (Fig. 7, left), which can give excitation energy of 4.0 eV, the total being sufficient for bandgap excitation. However, quantitative experiments and analyses have demonstrated that the nonlinear excitation can hardly occur under the present light intensity [32,33]. Alternatively, we can envisage some photo-electronic excitation processes which are unique to amorphous semiconductors having band-tail states. Such excitation processes may be analyzed through photocurrents. Actually, dependence of photocurrents in As_2S_3 upon the photon energy and light intensity manifests that the Urbach-edge light behaves as if it were bandgap light when the light intensity is higher than a certain level (see, Fig. 2), which corresponds to a complete occupation of localized states (trap filling) below 2.0 eV (~10^{17} /cm^3) [34]. Accordingly, it is plausible that a carrier excited to a state at 2.0 eV is further excited to a band through some means, such as two-step excitation (Fig. 7, center) [32] or multi-step thermal activation through band-edge states (Fig. 7, right) [35]. Then, the carrier may behave as if it were excited by bandgap illumination.

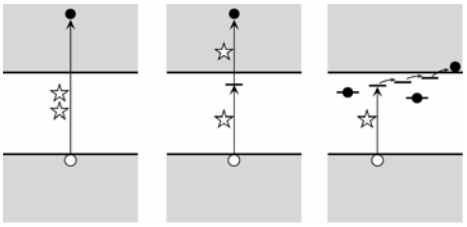

Fig. 7. Bandgap excitation by the conventional two-photon process (left), by two sub-gap photons through a tail state (two-step excitation) (center), and by a sub-gap photon and successive thermal activations through tail states (right).

4.2 Structural change

What kinds of atomic changes occur at the photo-expansion? Detailed x-ray diffraction measurements have shown a minute, but reproducible, photoinduced change (Fig. 8) at around the first sharp diffraction peak [23], which is located at ~12 nm^{-1} [3,4]. Although the origin of the peak remains to be ambiguous [3,4], the so-called distorted layer model [36] suggests that the detected change in x-ray profiles, which is an asymmmetric broadening of the peak, is a signature of *interlayer cracking* [23]. That is, as illustrated in Fig. 9c, in some regions (~1/100), the distance between As_2S_3 segmental layers increases from ~0.5 nm to ~1 nm.

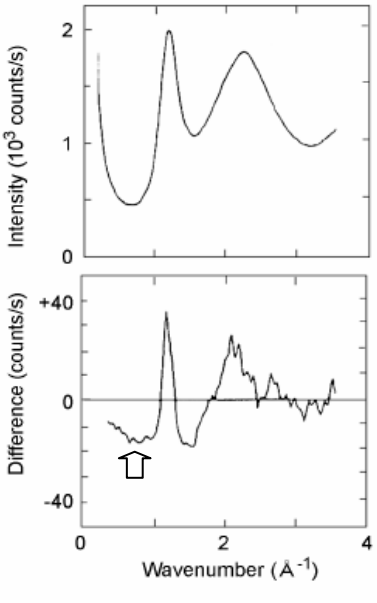

Fig. 8. An x-ray diffraction pattern of As_2S_3 glass (upper) and the photoinduced change (lower), in which positive differences mean intensity reductions. The arrow indicates an important change.

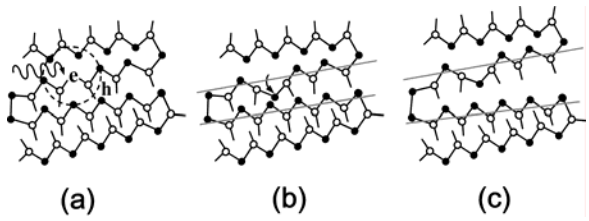

Fig. 9. Schematic illustrations (cross-sectional view) of microscopic expansion in As_2S_3 with a segmental layer structure consisting of As (open circles) and S (solid circles). (a) A photon excites a pair of electron and hole. (b) When the carriers are excited, atomic bond twisting of an S atom occurs [37], and then the carriers may recombine, producing a strong interlayer stress. (c) Stress relaxation occurs through interlayer expansion.

However, still speculative is the process connecting the electronic excitation and the structural change. Tanaka have proposed a successive atomic-motion model [23,24]. As illustrated in Fig. 9(a, b), the electronic excitation induces an atomic structural change such as bond twisting (with time scales of ps - ns) [37], a kind of disorder increases, which produces substantial interlayer stresses. Fig. 9(c) shows that this stress gives rise to successive interlayer relaxation (with time scales of μs - ms). These processes probably include creation of ESR-active defects, which is demonstrated in As_2S_3 at low temperatures under weak-light illumination [38]. Then, this microscopic expansion, which may occur in the interior of samples, is transferred to free surfaces (with time scales of s) with the *photoinduced fluidity*, which may occur through bond interchanges, as illustrated in Fig. 10 [26,31]. Note that this model for volume expansion is similar to the formation process of Schottky-type defects in alkali-halide crystals [1].

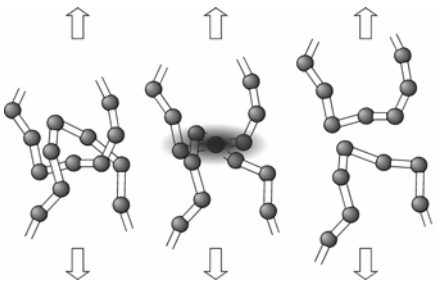

Fig. 10. Photoinduced bond interchanges in Se chains subjected to a stress along the vertical direction. Entangled chains produce a localized state (left), at which a photon is selectively absorbed, and a hybridized state is formed (center). Then, the lock may be released through bond interchange (right).

4.3. Remaining problems

The present photo-electro-structural model seems to be consistent with some observations. First, we see in the light-intensity dependence (Fig. 3) that the giant photo-expansion appears only when sufficient fluidity is attained ($\gtrsim 10^2$ W/cm^3). This result shows unambiguously that the photoinduced fluidity is a prerequisite for the giant photo-expansion, which is consistent to that the fluidity and the expansion are ascribed to different structural changes. That is, the fluidity occurs through interlayer slipping and bond interchange [26,31] and the expansive force is given by the interlayer expansion (Fig. 9). We also see in Fig. 3 that the photodarkening induced by sub-gap light also shows a marked enhancement at ~10^2 W/cm^3, which may be a manifestation of the unique excitation process discussed in 4.1. Second, the temperature dependence (Fig. 5) can be understood. That is, the structural disordering (bond twisting) is assumed to cause the photodarkening, which is known to become greater at lower temperatures [37]. Also, the photoinduced fluidity becomes more prominent at lower temperatures [26,31]. Therefore, the giant expansion can increase at low temperatures. Third, this model is consistent also with a pressure effect, which is a photodarkening increase under hydrostatic compression [39]. In the present model, since the expansion is suppressed by the compression, the interlayer stress (Fig. 9(b)) cannot be relaxed. Accordingly, the photodarkening becomes greater.

This model, however, needs further considerations. The most complicated point is the relationship between the carrier generation (Fig. 7), the microscopic expansion (Fig. 9), and the fluidity [26,31], the last being indispensable to transferring the microscopic expansion to surfaces. Since the fluidity appears at lower light intensities than those needed for the giant photo-expansion (Fig. 3), the fluidity may be a consequence of moderate trap excitation, which assists bond interchanges [26,31]. Some fluidity seems to be indispensable also for the conventional expansion by bandgap illumination. In addition to this qualitative problem, quantitative aspects are far from understandings. For instance, why is the degree of intrinsic volume expansion in As_2S_3 glass at room temperature ~0.5%?

On the other hand, Shimakawa et al. have proposed an electrical charging model [40-42]. That is, electron-hole pairs are photo-generated, and the holes immediately diffuse from an illuminated region, reflecting higher mobility [3,4]. Then, the illuminated region negatively charges in *macroscopic scales*, where Coulomb-type repulsive force causes a volume expansion. This idea can be regarded as a kind of electrical volume expansions, which have been proposed for micro-explosions upon irradiation of intense sub-ps lasers [43] and for volume expansions charged by electron beams [44]. In these models, the expansion and the fluidity are not distinguished. In a very recent work, Shimakawa et al. have reported that the photodarkening is affected by applications of static electric fields, and they emphasize that this observation reinforces their electrical model [42].

However, Shimakawas' model may also face to some problems [45]. For instance, it has been demonstrated that no one-to-one correspondence exists between the temporal growths of photodarkening and giant photo-expansion [23]. Accordingly, the electric-field effect does not necessarily support their electrical model. Or, the relation between the photodarkening and the photo-expansion is not clear in their model. In addition, their model appears to be in conflict with the temperature dependence (Fig. 5). At

lower temperatures, the expansion increases, while the hole diffusion becomes smaller [4], which implies that the electrical charging becomes smaller, giving rise to smaller expansions. In addition, their model may not explain the relationship between the fluidity and the giant photo-expansion, observed in the light-intensity dependence (Fig. 3). That is, in their model, the two changes are assumed to appear concomitantly, which is inconsistent with the observation. And, their model cannot explain a fact that, in some chalcogenide glasses as $Ge_1As_4Se_5$, *photo-contraction* appears exceptionally [10,23].

It may be fair to conclude that further studies are needed for the two models and also for other possibilities [24]. For obtaining deeper understandings, time-resolved structural studies may give valuable insights. In addition, the so-called first-principle computer simulations including at least 1000 atoms, which can cover several interlayer segments, will be valuable [46]. To the authors' knowledge, there are no simulations which show volume differences before and *after* illumination, although Hegedüs et al. have demonstrated an expansion in Se *during* illumination [47].

5. Applications

5.1. Perspective

Summarizing the features described above, we can expect that, upon illumination of moderate-intensity (~1 kW/cm^2) focused ($L/r > 1$) Urbach-edge light, many chalcogenide glasses exhibit prominent volume expansions accompanying refractive-index increases. For As_2S_3 exposed at room temperature, the apparent volume expansion and the refractive-index increase amount to ~5% and ~1%. When illuminated at low temperatures these changes still increase, while the changes probably relax very slowly at room temperature to steady values. These volume and optical changes provide an increase in the optical path length nL (n is the refractive index and L the sample thickness), which is useful for production of optical components. Note that in a photoinduced change providing a volume compaction ($\Delta L < 0$) and a refractive-index increase ($\Delta n > 0$), the modification of optical path lengths is not necessarily positive.

The giant expansion can produce micron-scale modifications. The expansion shape of modifications roughly replicates the intensity distribution of light spots employed, and the lateral dimension $2r$ can be varied at 5-50 μm. Here, the minimal dimension is governed by the size ($2r$) of focused light spots, which is limited by light diffraction. By using evanescent waves in optical probe microscopy, we may produce expansions of ~0.1 μm. On the other hand, the maximal size is governed by a necessary laser power, which must give the light intensity higher than ~1 kW/cm^2 (Fig. 3). Another prerequisite is that the sample thickness L must satisfy $L/r \gg 1$. Under these conditions, the giant expansion is promising for many applications as described below.

5.2. Micro-lens

A straightforward application of the giant photo-expansion is a micro-lens [12,48]. Just a light exposure can produce the lens, which is stable if it is used under weak or long-wavelength ($\hbar\omega \ll E_g$) illumination. If light is shed upon a sample through a pin hole, interference-affected expansions appear [48], which may be useful for special purposes. We can also produce an expansion which accompanies a dip at the center, Fig. 11. Lens arrays have been fabricated [48]. For producing a good lens, however, we need considerations between light-intensity profile, saturated expansion-form, and lens aberration.

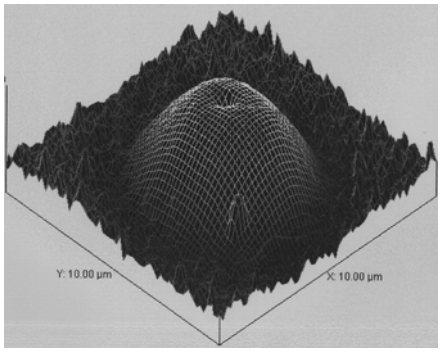

Fig. 11. An expansion (0.12μm high) with a central dip produced on a surface of an annealed As_2S_3 film (4 μm thick), which is deposited on a glass slide. The deformation, which manifests the expansion and the fluidity, has been produced as follows: First, an AFM cantilever is fixed at a position on the film. Then, the position is illuminated from the rear side through the substrate by focused 633 nm light for several minutes. After the illumination being switched off, the image is taken by scanning the cantilever.

Micro-lenses for optical fibers have been produced. Here, two features are effectively employed [49-51]. One is that a chalcogenide layer of interest can be prepared by vacuum evaporation or sputtering, which can afford the layer to be deposited on to spatially-restricted areas such as the end surface of optical fibers. The other is that, in the present method, the lens is positioned automatically on the fiber core, which is typically ~5 μm in diameter. This is because the volume expansion can be produced by light which can propagate through the fiber as a single transversal mode. Accordingly, the lens can be produced exactly upon the core of optical fibers. To demonstrate this idea, we have produced As_2S_3 micro-lenses for conventional oxide-glass optical fibers using 633 nm (2.0 eV) light (Fig. 12). The produced lens can focus transmitted light with wavelengths of 633 and 1047 nm. Anti-reflection coating using sputtered GeO_2 films has been demonstrated to be effective [50]. Following this method, we will be able to produce compound-eye lenses upon a bundle of fibers.

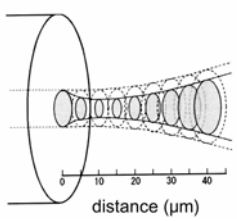

Fig. 12. Focusing characteristics of an As_2S_3 (10 μm thick) micro-lens fabricated on an end surface of an oxide-glass optical fiber with a core diameter of 6 μm [50]. The lens is formed by an exposure for 1 h to He-Ne laser light (~2 mW), which is coupled into the fiber at the other end. Dashed circles show light divergence before the lens is formed.

The present method may be more useful than other known two techniques. The most common technique is to assemble separated micro-lenses, but this needs naturally stringent positioning. A more sophisticated technique may be to follow a photolithographic process using conventional polymers [52-54]. However, the present method is superior, at least, in three points. First, the organic film must be prepared by spin-coating, which may not be suitable for such small areas as the fiber end. Second, it can be photo-processed with ultra-violet light, which may not propagate in oxide-glass fibers. Third, etching is needed for photo-polymers. However, in respect of production efficiencies, this photolithographic technique may be superior.

Saitoh and Tanaka have produced aspherical micro-lenses for semiconductor lasers, Fig. 13 [55]. As is known, a semiconductor laser emits a divergent beam, and accordingly, an aspherical lens or a lens assembly are needed for collimation or focusing [56,57]. In addition, the conventional edge-emitting laser diodes provide ellipsoidal beams, which should be transformed to circular spots for coupling to optical components such as optical fibers, which have circular symmetries. However, the lens alignment is again stringent due to the small laser size of ~10 μm.

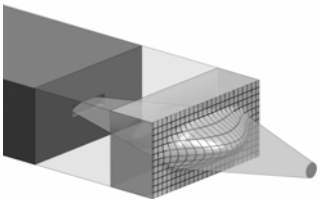

Fig. 13. Principle of a monolithic-type self-developing aspherical micro-lens (right) with a semiconductor laser (left) and a spacer (middle) [58]. An ellipsoidal beam from the laser is transformed to a circular spot.

Suppose an As_2S_3 layer, which is fixed to a semiconductor laser with some means, is illuminated by the laser beam. If the light is red and intense, the As_2S_3 layer expands aspherically, reflecting an ellipsoidal laser beam. Then, if the layer thickness and position have been adjusted appropriately, the expansion can work automatically as an ellipsoidal-to-spherical conversion lens. Such an idea has been demonstrated using As_2S_3 layers (10-50 μm thick) and semiconductor lasers emitting 660 nm (1.9 eV) light [55]. The lens produces circular spots (~1 μm in diameter) at focal distances of 10-80 μm. This idea can be extended to other lasers emitting different wavelengths using other chalcogenide glasses, such as As_2Se_3 for near infrared light and GeS_2 for blue light (see, Section 2) [58].

5.3. Other applications

Linear expansions are also useful, which can be produced by moving samples under light illumination or by illumination through slits. Cylindrical lenses have been produced [48]. The linear expansion will work as channeled waveguides, since the expansion accompanies the refractive-index increase. Relief-type gratings have also been fabricated [59,60].

In addition, replicas having depressions may be produced by using expanded samples as masters, a process being demonstrated for etched chalcogenide films previously [61]. Nevertheless, the present one-step photo-production method is competitive to photolithographic techniques [62,63] and to electron-beam modifications [44].

6. Final remarks

The chalcogenide glass can be regarded as a kind of amorphous semiconductors. Since it is a semiconductor with optical energy gap of 1-3 eV, the glass can be excited by visible light. Since the atomic structure is disordered, the electronic excitation is spatially localized, which is likely to produce strong electron-lattice interaction. And lastly, since the glass is thermo-dynamically meta-stable, it can be altered to other quasi-stable atomic configurations.

In addition, the structure is important. Many chalcogenide glasses have two-dimensional structures consisting of two kinds of atomic bonds, i.e. covalent and van-der-Waals types. Accordingly, the network has an intermediate rigidity between those in organic polymers (one-dimensional) and oxide glasses (three-dimensional), the both having wider bandgap energies if not sensitized by dyes. Because of this intermediate structure and the appropriate bandgap energy, the chalcogenide glass exhibits relatively-high photo-sensitivity with practical stability. And, among the three chalcogenides (S, Se, and Te), the sulfide such as As_2S_3 and GeS_2 possesses the greatest photostructural changes [64], probably because of the most prominent dual bonding structure.

The giant photo-expansion may be the most dramatic among many photoinduced changes in the chalcogenide glasses. To the author's knowledge, in all solids, there are no comparable phenomena in which such a great volume expansion appears just with visible light exposures. Therefore, the application is promising.

Acknowledgements

We would like to dedicate this article to a giant, Professor Dr. Doc. Radu Grigorovici, now celebrating his 95th birthday, who has given many exciting ideas into the challenging field of amorphous solids.

References

[1] N. Itoh, A. M. Stoneham, Materials Modification by Electronic Excitation (Cambridge University Press, Cambridge, 2001).
[2] G. P. Agrawal, Applications of Nonlinear Fiber Optics (Academic Press, San Diego, 2001) Chap. 1.
[3] M. A. Popescu, Non-Crystalline Chalcogenides (Kluwer Academic Publishers, Dordrecht, 2000).
[4] J. Singh, K. Shimakawa, Advances in Amorphous Semiconductors (Taylor & Francis, London, 2003).
[5] A. V. Kolobov (Ed.), Photo-Induced Metastability in Amorphous Semiconductors (Wiley-VCH, Weinheim, 2003).
[6] G. Lucovsky, M. Popescu (Eds.), Non-Crystalline Materials for Optoelectronics (INOE, Bucharest-Magurele, 2004).
[7] M. Kasai, H. Nakatsui, Y. Hajimoto, J. Appl. Phys. **45,** 3209 (1974).
[8] J. P. De Neufville, S. C. Moss, S. R. Ovshinsky, J. Non-Cryst. Solids **13,** 191 (1973/74).
[9] H. Hamanaka, K. Tanaka, A. Matsuda, S. Iizima, Solid State Commun. **19,** 499 (1976).
[10] K. Tanaka, J. Non-Cryst. Solids **35&36,** 1023 (1980).
[11] K. Tanaka, Y. Ohtsuka, J. Appl. Phys. **49,** 6132 (1978).
[12] H. Hisakuni, K. Tanaka, Appl. Phys. Lett. **65,** 2925 (1994).
[13] A. Saliminia, T.V. Galstian, A. Villeneuve, Phys. Rev. Lett. **85,** 4112 (2000).
[14] K. Tanaka, J. Optoelectron. Adv. Mater. **7,** 2571 (2005).
[15] K. Tanaka, H. Asao, Jpn. J. Appl. Phys. **45,** 1668 (2006).
[16] K. Tanaka, T. Gotoh, H. Hayakawa, Appl. Phys. Lett. **75,** 2256 (1999).
[17] K. Tanaka, H. Hisakuni, J. Non-Cryst. Solids **198-200,** 714 (1996).
[18] K. Tanaka, Philos. Mag. Lett. **79,** 25 (1999).
[19] K. Tanaka, J. Non-Cryst. Solids **352,** 2580 (2006).
[20] G. Beadie, W. S. Rabinovich, J. Sanghera, I. Aggarwal, Opt. Commun. **152,** 215 (1998).
[21] V. K. Tikhomirov, M. Barj, S. Turrell, Philos. Mag. Lett. **85,** 325 (2005).
[22] P. Lucas, E. A. King, A. Doraiswamy, J. Optoelectron. Adv. Mater. **8**, 776 (2006).
[23] K. Tanaka, Phys. Rev. B **57,** 5163 (1998).
[24] K. Tanaka, in: A. Andriesh and M. Bertolotti (Eds.) Physics and Applications of Non-Crystalline Semiconductors in Optoelectronics (Kluwer Academic Publishers, Dordrecht, 1997) p. 31.
[25] K. Tanaka, J. Non-Cryst. Solids **266-269,** 889 (2000).
[26] K. Tanaka, C. R. Chimie **5,** 805 (2002).
[27] K. Tanaka, N. Nemoto, H. Nasu, Jpn. J. Appl. Phys. **42,** 6748 (2003).
[28] N. Terakado, K. Tanaka, J. Non-Cryst. Solids **251,** 54 (2005).
[29] R. Sramek, F. Smektala, W. X. Xie, M. Douay, P. Niay, J. Non-Cryst. Solids **277,** 39 (2000).
[30] H. Hisakuni, K. Tanaka, Science **270,** 974 (1995).
[31] K. Tanaka, in: Ref. 5, p. 69.
[32] K. Tanaka, Appl. Phys. Lett. **80,** 177 (2002).
[33] K. Tanaka, Philos. Mag. Lett. **84,** 601 (2004).
[34] K. Tanaka, Appl. Phys. Lett. **73,** 3435 (1998).
[35] For n-step thermal excitation, the relative probability may be proportional to $\sim\{\exp(-0.4/0.025n)\}$, provided that downwards hopping is suppressed due to occupied localized states. For $n = 2$, this becomes 10^{-4}, much greater than 10^{-7}.
[36] K. Tanaka, Jpn. J. Appl. Phys. **37,** 1747 (1998).
[37] K. Tanaka, Jpn. J. Appl. Phys. **25,** 779 (1986).
[38] J. A. Freitas, Jr., U. Strom, S.G. Bishop, Phys. Rev. B **35,** 7780 (1987).
[39] K. Tanaka, Phys. Rev. B **30,** 4549 (1984).
[40] K. Shimakawa, N. Yoshida, A. Ganjoo, Y. Kuzukawa, Philos. Mag. Lett. **77,** 153 (1998).
[41] K. Shimakawa, in: Ref. 5, p. 58.
[42] K. Shimakawa, J. Optoelectron. Adv. Mater. **7,** 145 (2005).
[43] E.N. Glezer, E. Mazur, Appl Phys. Lett. **71,** 882 (1997).
[44] T. Tanaka, Appl. Phys. Lett. **70,** 261 (1997).
[45] E.V. Emelianova, G.J. Adriaenssens, V.I. Arkhipov, Philos. Mag. Lett. **84,** 47 (2004).
[46] D. A. Drabold, X. Zhang, J. Li, in: Ref. 5, p. 260.
[47] J. Hegedüs, K. Kohary, D. G. Pettifor, K. Shimakawa, S. Kugler, Phys. Rev. Lett. **95**, 206803 (2005).
[48] H. Hisakuni, K. Tanaka, Opt. Lett. **29,** 958 (1995).
[49] A. Saitoh, T. Gotoh, K. Tanaka, Opt. Lett. **25,** 1759 (2000).
[50] A. Saitoh, T. Gotoh, K. Tanaka, J. Non-Cryst. Solids **299-302,** 299 (2002).
[51] Japan Patent: 3531232.
[52] L. G. Cohen, M.V. Schneider, Appl. Opt. **13,** 89 (1974).
[53] B. G. Healey, S. E. Foran, D. R. Walt, Science **269,** 1078 (1995).
[54] M. Sasaki, T. Ando, S. Nogawa, K. Hane, Jpn. J. Appl. Phys. **41,** 4350 (2002).
[55] A. Saitoh, K. Tanaka, Appl. Phys. Lett. **83,** 1725 (2003).
[56] S. Sinziner, K.H. Brenner, J. Moisel, T. Spick, M. Testorf, Appl. Opt. **34,** 6626 (1995).
[57] Y. Fu, N.K.A. Bryan, IEEE Trans. Semicond. Manufac. **15,** 2 (2002).
[58] U.S. Patent: 7038247.
[59] S. Ramachandran, J. C. Pepper, D.J. Bray, S. G. Bishop, J. Lightwave Technol. **15,** 1371 (1997).
[60] A. Saliminia, T. Galstian, A. Villeneuve, K. Le Foulgoc, K. Richardson, J. Opt. Soc. Am. B **17,** 1343 (2000).
[61] T. Sakai, Opt. Commun. **24,** 47 (1978).
[62] N. P. Eisenberg, M. Klebanov, V. Lyubin, M. Manevich, S. Noach, J. Optoelectron. Adv. Mater. **2,** 147 (2000).
[63] D. Savastru, S. Miclos, R. Savastru, J. Optoelectron. Adv. Mater. **8,** 1165 (2006).
[64] K. Tanaka, J. Non-Cryst. Solids **59&60,** 925 (1983).

*Corresponding author: keiji@eng.hokudai.ac.jp (Ovshinsky Prize, 2001)